DNP-Enhanced Ultrawideline ^{207}Pb Solid-State NMR Spectroscopy: An Application to Cultural Heritage Science

Takeshi Kobayashi[1], Frédéric A. Perras[1], Anna Murphy[2], Yao Yao[2], Jaclyn Catalano[3], Silvia A. Centeno[4], Cecil Dybowski[2], Nicholas Zumbulyadis[5*] and Marek Pruski[1,6*]

[1]US DOE, Ames Laboratory, Ames IA, USA, 50011
[2]Department of Chemistry and Biochemistry, University of Delaware, Newark DE, USA, 19716
[3]Department of Chemistry and Biochemistry, Montclair State University, Montclair NJ, USA, 07043
[4]The Metropolitan Museum of Art, New York NY, USA, 10028
[5]Independent Researcher, Rochester NY, USA
[6]Department of Chemistry, Iowa State University, Ames, IA, USA 50011

Abstract:

Dynamic nuclear polarization (DNP) is used to enhance the (ultra)wideline ^{207}Pb solid-state NMR spectra of lead compounds of relevance in the preservation of cultural heritage objects. The DNP SSNMR experiments enabled, for the first time, the detection of the basic lead carbonate phase of the lead white pigment by ^{207}Pb SSNMR spectroscopy. Variable-temperature experiments revealed that the short T_2' relaxation time of the basic lead carbonate phase hinders the acquisition of the NMR signal at room temperature. We additionally observe that the DNP enhancement is twice as large for lead palmitate (a lead soap, which is a degradation product implicated in the visible deterioration of lead-based oil paintings), than it is for the basic lead carbonate. This enhancement has allowed us to detect the formation of a lead soap in an aged paint film by ^{207}Pb SSNMR spectroscopy; which may aid in the detection of deterioration products in smaller samples removed from works of art.

Introduction

Lead white, which consists of primarily basic lead carbonate, $2PbCO_3 \bullet Pb(OH)_2$, was one of the first artificially produced pigments in antiquity and the white colorant of choice in paintings until recently. The earliest known recorded recipe for its preparation was by Theophrastus around 300 BCE.[1] Unfortunately, lead white, as well as other lead-based pigments such as lead-tin yellow type I, react with free fatty acids produced by the hydrolysis of oil-based binders in the paintings to form lead soaps (lead carboxylates). These soaps subsequently develop into aggregates that gradually grow as the painting ages and eventually protrude through the paint surface, leading to the deterioration of many iconic world cultural heritage objects. Therefore, the formation of these compounds, such as lead palmitate, for example, is a major concern in the conservation of oil-based paintings.

Minimally invasive techniques, such as FTIR and chromatographic methods, which require the removal of μg-to-mg amounts of sample from the artwork, are acceptable in most archaeological contexts. In the analysis of artistic materials and their deterioration products, non-invasive analytical techniques such as Raman spectroscopy[2, 3] or X-ray fluorescence are generally preferred. Solid-state nuclear magnetic resonance (SSNMR) spectroscopy is capable of providing unique atomistic insights into cultural heritage objects;[4, 5] however, the inherently low sensitivity impedes its use for the structural characterization of low-concentration components that often significantly impact material properties. Recent progress in dynamic nuclear polarization (DNP), including instrumental improvements,[6-9] the introduction of biradical polarizing agents,[10-13] and advances in theory,[14, 15] have impressively enhanced SSNMR's sensitivity, especially in the area of materials science. Indeed, DNP has enabled the observation of species at low concentrations that were not accessible by conventional SSNMR in

biomolecules, in polymers, and on the surfaces of catalysts, to cite a few examples, raising the possibilities for applications in other areas such as cultural heritage science.[16-21]

Aside from the issues arising from low concentration, heavy spin-1/2 nuclei, such as ^{207}Pb found in pigments, typically possess chemical shift anisotropies (CSA) that may be as large as several thousand ppm, further exacerbating the sensitivity problem. Although magic-angle spinning (MAS) may be applied to average the effects of large CSAs, in ultrawideline cases, and particularly in amorphous materials, large manifolds of unresolved spinning sidebands are typically obtained.

The experimental difficulties are further compounded by the limited excitation bandwidths of square RF pulses. A solution to this issue was, however, proposed in 2007 by Bhattacharyya and Frydman,[22] who used frequency-swept wideband, uniform-rate, and smooth-truncation (WURST) pulses[23] for the excitation and refocusing of wideline spectra. O'Dell and Schurko demonstrated that the sensitivity of this approach could be further enhanced by acquiring a spectrum with a WURST-based Carr-Purcell-Meiboon-Gill (WCPMG) train of echoes.[24] Subsequently, Harris and coworkers developed a broadband adiabatic inversion cross-polarization (BRAIN-CP) sequence and combined it with WCPMG acquisition (BRAIN-CP-WCPMG), herein denoted as BCP for brevity.[25] Finally, these developments have been coupled with DNP for the sensitivity-enhanced acquisition of ultrawideline spectra.[26] The feasibility of the DNP-BCP approach has been demonstrated for ^{195}Pt{^{1}H} SSNMR in platinum-containing metal-organic frameworks[26] and for ^{35}Cl{^{1}H} SSNMR in pharmaceuticals.[27] Here, we use ^{207}Pb{^{1}H} DNP-BCP, ^{207}Pb{^{1}H} DNP-CPMAS and ^{207}Pb WCPMG as tools for elucidating the degradation mechanism of lead-based pigments in paint films.[4, 5, 28] Our results demonstrate that

this new methodology holds promise for the application of SSNMR to dilute and severely mass-limited archaeomaterials and other objects of cultural significance.

Materials and methods

Samples. The samples chosen for this study included lead white, a model lead soap (lead palmitate), and an aged paint film. 'Basic lead carbonate' was used as purchased from Sigma Aldrich. Lead palmitate was prepared by methods adapted from published protocols.[29-31] Briefly, lead nitrate in water was mixed with an equimolar amount of palmitic acid in ethanol and potassium hydroxide and reacted for 20 minutes at 80°C. The mixture was cooled, filtered, and washed with water, methanol, ethanol, and acetone. The paint film was prepared by mixing lead white with 22% linseed oil by weight. The paint was spread on glass slides and cured at room temperature for 3 months before it was scraped off and kept in a sealed clear jar under laboratory conditions for 4 years. Before the NMR measurements, the aged sample was ground under liquid nitrogen.

SSNMR measurements. All SSNMR experiments were performed at 9.4 T (400 MHz for ^{1}H and 83.7 MHz for ^{207}Pb) on a Bruker Biospin AVANCE III DNP-SSNMR spectrometer, equipped with a 263 GHz gyrotron and a low-temperature MAS probe. The samples were wet with a 16 mM solution of the TEKPol biradical[32] in a 1,1,2,2-tetrachloroethane:methanol-d4 96:4 mixture, and packed in 3.2-mm sapphire rotors with an active sample volume of ~25 µl. Static wideline ^{207}Pb{^{1}H} DNP-BCP experiments were performed at a temperature of 110 ± 5 K. ^{207}Pb{^{1}H} DNP-CPMAS spectra were measured at 105 ± 5 K. Conventional (non-DNP) static ^{207}Pb WCPMG experiments were carried out at several temperatures ranging from 110 K to 308 K. The chemical shifts were referenced to $Pb(Me)_4$ at room temperature using a solution of DSS

(4,4-dimethyl-4-silapentane-1-sulfonic acid) and the universal referencing scale.[33] Detailed experimental conditions are given in the figure captions.

Results and discussion

Lead white. Despite the importance of the basic lead carbonate, its crystal structure has only recently been solved using powder X-ray diffraction data.[34] It was found to consist of two distinct hexagonal layers of Pb atoms (labeled A and B), stacked along [001] in a $[BAA]_n$ arrangement, where layer A is composed of Pb (Pb1 site) and CO_3, and layer B is composed of Pb (Pb2 site) and OH. Consequently, there are twice as many Pb1 sites as Pb2 sites.

Previous attempts to study the structure of lead white (containing mainly the basic lead carbonate) by ^{207}Pb SSNMR have been unsuccessful. Typically, only the significant (often up to 15% by weight) lead carbonate impurity is observed. This phase is easily detected at room temperature by directly excited MAS[35] spectroscopy, as well as by static[36] ^{207}Pb SSNMR experiments, due to its relatively small CSA (see Figure 1c) and has been erroneously identified as originating from the carbonate layer of the basic lead carbonate.[35]

The ^{207}Pb DNP-BCP spectrum of lead white is shown in Figure 1a. The spectrum spans more than 5000 ppm, and has been be acquired in a piecewise manner using the variable offset cumulative spectrum (VOCS) method.[37] In agreement with the crystallographic data for the basic lead carbonate, the spectrum is well reproduced when fit to two sites, having distinct chemical shift parameters (Figure 1a and Table 1), with an intensity ratio of roughly 2:1. From this intensity ratio the two components are straightforwardly assigned to the abovementioned Pb1 (lead carbonate layer, A) and Pb2 (lead hydroxide layer, B) sites in the crystal structure. These two sites feature different cross-polarization rates, which reflect their respective

proximities to hydrogen atoms. Although the precise hydrogen positions are currently unknown, the Pb2 sites are expected to reside closer to the hydroxyl moieties than the Pb1 sites (The relevant Pb1–O and Pb2–O distances were reported at 2.36 Å and 1.95 Å, respectively.[34]) and are thus expected to have faster CP kinetics. The BCP signal intensities as a function of the contact time, measured for the highest-intensity singularity for each site, are shown in Figure 2. The CP build-up rate is faster for Pb2, further supporting the signal assignment.

The relatively low DNP enhancement factor of $\varepsilon \sim 4$, estimated by comparing the signal intensity in the presence and absence of microwave irradiation (Figure 1b), is caused by the difficulty to satisfy the cross-effect condition in static samples,[15, 26] and the non-porous nature of the material, which forces us to rely on spin diffusion to polarize the bulk of the particles.[38-40] We further note that the use of a ^{207}Pb{^{1}H} CPMAS technique, both with and without the application of microwaves, suppresses the signals from ^{207}Pb nuclei in hydrogen-free regions of the sample, namely lead carbonate. In agreement with previous work, this lead carbonate phase is readily detected by a ^{207}Pb WCPMG experiment (Figure 1c), carried out at 308 K using a conventional direct-excitation scheme without the application of DNP. Interestingly, our attempts to perform a similar BCP measurement at 308 K yielded no signal for either phase.

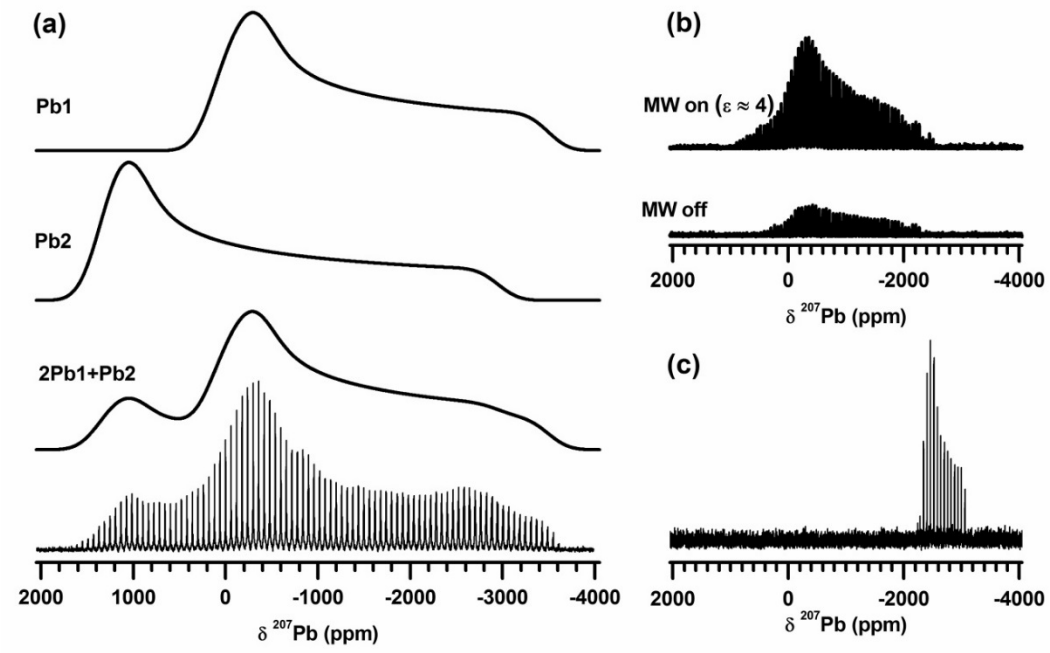

Figure 1. ^{207}Pb SSNMR spectra of lead white. (a) ^{207}Pb{^{1}H} DNP-BCP spectrum (bottom) and its simulated decomposition into signals assigned to the Pb1 and Pb2 sites. The adiabatic inversion (CP) pulse swept over 250 kHz for a period of 20 ms while the refocusing CPMG pulses lasted 50 μs and swept over 500 kHz. The experimental line shape is composed of eight subspectra, each measured with 64 scans and a recycle delay of 6 s. A 20 kHz Gaussian broadening was applied to the simulated spectra. A single subspectrum acquired with and without the application of microwaves is shown in (b). (c) ^{207}Pb WCPMG spectrum featuring solely the lead carbonate resonance. This spectrum was acquired at 308 K, using 128 scans and a recycle delay of 8 s.

Table 1. ^{207}Pb Chemical Shift Tensor Components of the Basic Lead Carbonate, Determined at 105 K

Pb-site	δ_{11} (ppm)[a]	δ_{22} (ppm)[a]	δ_{33} (ppm)[a]	δ_{iso} (ppm)	Ω (ppm)	κ
Pb1	160	-310	-3500	-1216	3660	0.74
Pb2	1400	1050	-2950	167	4350	0.84

[a]The uncertainty in each tensor component (δ_{11}, δ_{22}, and δ_{33}; which are ordered as: $\delta_{11} \geq \delta_{22} \geq \delta_{33}$) is estimated to be ~10 ppm, which gives an estimated uncertainty in the isotropic shift (δ_{iso} =

($\delta_{11}+\delta_{22}+\delta_{33}$)/3) of ~10 ppm. The estimated uncertainty in the span ($\Omega \approx \delta_{11} - \delta_{33}$) is ~14 ppm. The uncertainty in the skew ($\kappa \approx 3(\delta_{22} - \delta_{22})/\Omega$) is ~ 0.03.

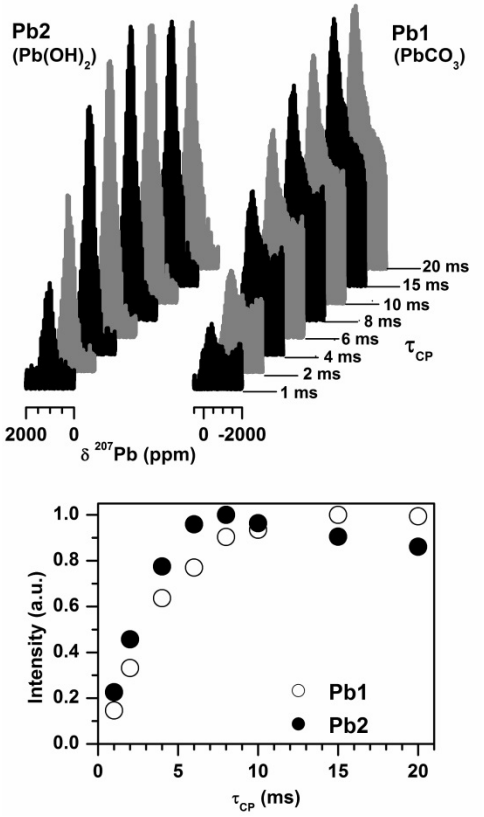

Figure 2. The ^{207}Pb{^{1}H} DNP-BCP build-up curves as a function of the CP contact time, measured for the Pb1 and Pb2 sites at 110 K.

To explain the puzzling disappearance of the basic lead carbonate signals around room temperature, we collected a series of ^{207}Pb WCPMG spectra at five temperatures ranging from 110 K to 308 K (Figure 3a). As the temperature is elevated, the spikelets from the lead white phase broaden and eventually disappear in the baseline, demonstrating that the lack of signal is due to a decrease of the T_2' relaxation time of the Pb1 and Pb2 sites. Concurrently, the line width of the ^{1}H signal decreases with increasing temperature (Figure 3b), suggesting that the accelerated decoherence of the ^{207}Pb magnetization is attributable to increased mobility in the solid.[41] A possible way to detect both the basic lead carbonate and lead carbonate signals in a

single experiment might be the measurement of the conventional ^{207}Pb WCPMG spectrum at low temperature using a biradical-free sample (direct DNP is not feasible here). We have determined, however, that the sensitivity of such an experiment is much lower than that of a DNP-BCP experiment (for Pb1 and Pb2 by a factor of ~30, in terms of experimental time), making it impractical for size-limited samples.

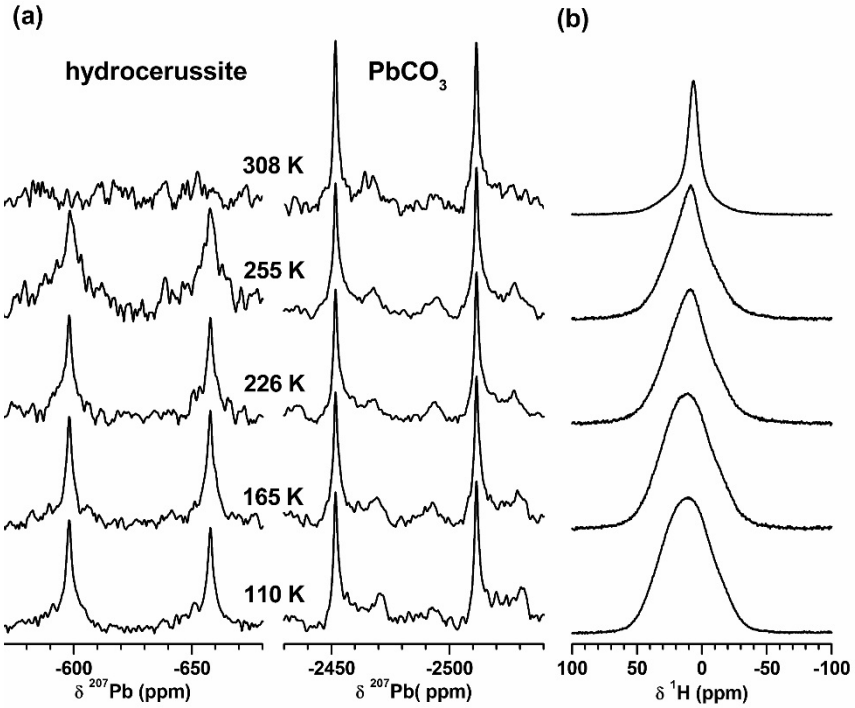

Figure 3. Sections of the ^{207}Pb WCPMG (a) and ^{1}H spin echo (b) spectra of lead white measured at different temperatures. All ^{207}Pb spectra were obtained using the same conditions as in Figure 1, with a recycle delay of 15 s and a greater number of scans: 256 scans at 110 K, 165 K, and at 308 K, 512 scans at 226 K, and 768 scans at 255 K. The ^{1}H spin echo spectra were obtained under a static condition, with a half-echo period of 50 μs, a recycle delay of 15 s and 16 scans. The spectra in each column (with the exception of basic lead carbonate at 308 K) were normalized to constant height to eliminate the effect of the varying numbers of scans, Boltzmann polarizations, T_1 relaxation times and RF efficiencies at the different temperatures.

Lead soaps. We first assessed the performance of DNP on a typical lead soap: lead palmitate ($C_{32}H_{62}O_4Pb$). The DNP-enhanced $^{207}Pb\{^1H\}$ CPMAS and BCP spectra of lead palmitate are shown in Figure 4, along with their corresponding simulated spectra based on the previously published chemical shift tensor parameters.[31] The smaller span of the Pb palmitate resonance (740 ±4 ppm), as compared to that of lead white and other Pb alkanoates,[31] enables the performance of CPMAS to be assessed alongside BCP.

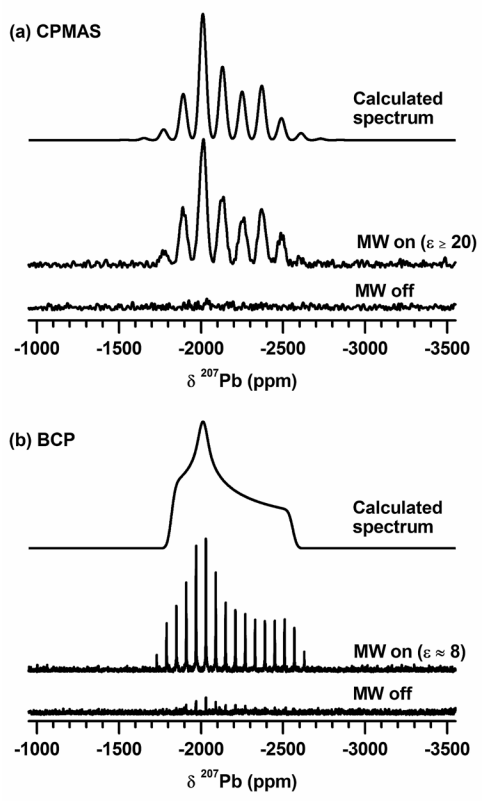

Figure 4. $^{207}Pb\{^1H\}$ CPMAS (a) and $^{207}Pb\{^1H\}$ BCP (b) spectra of lead palmitate, acquired with microwave radiation on and off. In contrast to lead white, the spectra could be easily acquired without stepping the carrier frequency. Simulated lines for the DNP-CPMAS and DNP-BCP spectra are shown at the top. In (a) the MAS rate was set to ν_R = 10 kHz, the contact time to 10 ms, and 256 scans were acquired with a recycle delay of 8 s; in (b) the adiabatic pulses used for CP and CPMG refocusing were the same as those used for lead white, and 64 scans were acquired with a recycle delay of 8 s.

Both experiments lead to sizeable enhancements of the ^{207}Pb SSNMR spectra. The observed enhancement factors are $\varepsilon \geq 20$ and $\varepsilon \approx 8$ for the CPMAS and BCP experiments, respectively. The lower enhancement factor observed in the static sample is caused by the reasons discussed previously. Importantly, the enhancement factor is approximately a factor of 2 greater for the lead soap than it is for lead white, which can, at least in part, be attributed to the higher proton density of the alkyl chain compared to the $Pb(OH)_2$ layer.

Previous attempts at observing the formation of lead soaps in aged paint films using ^{207}Pb SSNMR were unsuccessful, primarily due to the low amounts of lead soaps present as well as the aforementioned lead carbonate impurity. DNP-BCP may be the ideal ^{207}Pb SSNMR technique for this application, given that 1) it completely suppresses the signal from the lead carbonate phase and 2) it selectively enhances the signal from the lead soap.

Accordingly, we measured the ^{207}Pb{^{1}H} DNP-BCP spectrum of a lead white/linseed oil (78/22 wt%) paint film that had been aged for four years at ambient temperature and relative humidity (Figure 5a). This process mimics the natural aging process of lead oil paints. The aged film primarily displays the spectrum of basic lead carbonate, with a superimposed signal that we assign to decomposition products. By subtracting the spectrum of lead white from that of the aged film, the spectrum of the decomposition products can be isolated (Figure 5b). Although a large fraction of that signal is attributable to lead carbonate, that may now be detectable by CP due to the proton-rich oil matrix, small additional contributions are still discernible (indicated by the grey arrow in Figure 5b) which agree with the CS tensor parameters of Pb palmitate (see Figure 4) and other lead carboxylates.[4] Although this weak signal does not allow a definitive

assignment, its position and breadth suggests the formation of long-chain lead carboxylates during the paint aging process.

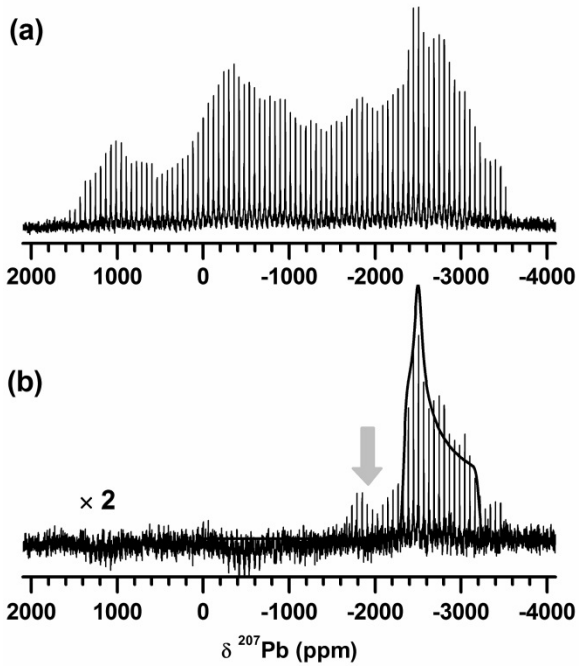

Figure 5. (a) $^{207}Pb\{^{1}H\}$ DNP-BCP spectrum of aged paint film measured at 108 K. The spectrum in (b) is the result of subtracting the signals from lead white, thus revealing the signal from the decomposition products; the arrow shows the signal corresponding to a lead soap. The pulse parameters were identical to those used for lead white, *vide supra*.

Conclusion

We have carried out DNP-enhanced ^{207}Pb SSNMR measurements, which have allowed us to observe, for the first time, ^{207}Pb SSNMR signals from the basic lead carbonate phase in the lead white pigment. In agreement with crystallographic data, the spectral fitting reveals the existence of two Pb sites with an intensity ratio of 2:1, corresponding to the carbonate and hydroxide layers. Additionally, we observed that the DNP enhancement in a typical lead soap (lead palmitate) is twice as large as that for basic lead carbonate, which facilitates its detection in aged

paint films. We have used this new methodology to detect, also for the first time, the formation of a lead soap in an aged paint film by ^{207}Pb SSNMR spectroscopy. These insights could not have been obtained by conventional SSNMR methodology.

Acknowledgements

This research is supported by the U.S. Department of Energy, Basic Energy Sciences, Division of Chemical Sciences, Geosciences, and Biosciences through the Ames Laboratory. Partial support for F.P. is through a Spedding Fellowship funded by the Laboratory Directed Research and Development (LDRD) program at the Ames Laboratory. Ames Laboratory is operated for the DOE by Iowa State University under Contract No. DE-AC02-07CH11358. F.P. also thanks NSERC (Natural Sciences and Engineering Research Council of Canada) and the Government of Canada for a Banting Postdoctoral Fellowship. The research was supported by the National Science Foundation under Grants CHE-1139192 and DMR-1608366 to University of Delaware, and CHE-1139180 and DMR-1608594 to The Metropolitan Museum of Art.

References

1 E. R. Caley and J. C. Richards, *Theophrastus on Stones*, The Ohio State University Press, Columbus, 2016.
2 P. Vandenabeele, H. G. M. Edwards and L. Moens, *Chem. Rev.*, 2007, **107**, 675-686.
3 S. A. Centeno, *J. Raman Spectrosc.*, 2016, **47**, 9-15.
4 J. Catalano, A. Murphy, Y. Yao, G. P. A. Yap, N. Zumbulyadis, S. A. Centeno and C. Dybowski, *Dalton Trans.*, 2015, **44**, 2340-2347.
5 J. Catalano, A. Murphy, Y. Yao, F. Alkan, N. Zurnbulyadis, S. A. Centeno and C. Dybowski, *J. Phys. Chem. A*, 2014, **118**, 7952-7958.
6 L. R. Becerra, G. J. Gerfen, B. F. Bellew, J. A. Bryant, D. A. Hall, S. J. Inati, R. T. Weber, S. Un, T. F. Prisner, A. E. McDermott, K. W. Fishbein, K. E. Kreischer, R. J. Temkin, D. J. Singel and R. G. Griffin, *J. Mag. Reson. A*, 1995, **117**, 28-40.
7 C. D. Joye, R. G. Griffin, M. K. Hornstein, K. N. Hu, K. E. Kreischer, M. Rosay, M. A. Shapiro, J. R. Sirigiri, R. J. Temkin and P. P. Woskov, *IEEE Trans. Plasma Sci.* 2006, **34**, 518-523.

8 A. B. Barnes, M. L. Mak-Jurkauskas, Y. Matsuki, V. S. Bajaj, P. C. A. van der Wel, R. DeRocher, J. Bryant, J. R. Sirigiri, R. J. Temkin, J. Lugtenburg, J. Herzfeld and R. G. Griffin, *J. Magn. Reson.*, 2009, **198**, 261-270.
9 M. Rosay, J. C. Lansing, K. C. Haddad, W. W. Bachovchin, J. Herzfeld, R. J. Temkin and R. G. Griffin, *J. Am. Chem. Soc.*, 2003, **125**, 13626-13627.
10 A. Zagdoun, G. Casano, O. Ouari, M. Schwarzwalder, A. J. Rossini, F. Aussenac, M. Yulikov, G. Jeschke, C. Coperet, A. Lesage, P. Tordo and L. Emsley, *J. Am. Chem. Soc.*, 2013, **135**, 12790-12797.
11 C. Sauvee, M. Rosay, G. Casano, F. Aussenac, R. T. Weber, O. Ouari and P. Tordo, *Angew. Chem. Int. Ed.*, 2013, **52**, 10858-10861.
12 C. S. Song, K. N. Hu, C. G. Joo, T. M. Swager and R. G. Griffin, *J. Am. Chem. Soc.*, 2006, **128**, 11385-11390.
13 K. N. Hu, H. H. Yu, T. M. Swager and R. G. Griffin, *J. Am. Chem. Soc.*, 2004, **126**, 10844-10845.
14 T. Maly, G. T. Debelouchina, V. S. Bajaj, K.-N. Hu, C.-G. Joo, M. L. Mak-Jurkauskas, J. R. Sirigiri, P. C. A. van der Wel, J. Herzfeld, R. J. Temkin and R. G. Griffin, *J. Chem. Phys.*, 2008, **128**, 052211.
15 K. R. Thurber and R. Tycko, *J. Chem. Phys.*, 2012, **137**.
16 V. K. Michaelis, E. Markhasin, E. Daviso, J. Herzfeld and R. G. Griffin, *J. Phys. Chem. Lett.*, 2012, **3**, 2030-2034.
17 O. Ouari, P. Trang, F. Ziarelli, G. Casano, F. Aussenac, P. Thureau, D. Gigmes, P. Tordo and S. Viel, *ACS Macro Lett.*, 2013, **2**, 715-719.
18 A. J. Rossini, A. Zagdoun, M. Lelli, A. Lesage, C. Coperet and L. Emsley, *Acc. Chem. Res.*, 2013, **46**, 1942-1951.
19 F. A. Perras, T. Kobayashi and M. Pruski, *J. Am. Chem. Soc.*, 2015, **137**, 8336-8339.
20 T. Kobayashi, F. A. Perras, I. I. Slowing, A. D. Sadow and M. Pruski, *ACS Catal.*, 2015, **5**, 7055-7062.
21 A. R. Mouat, C. George, T. Kobayashi, M. Pruski, R. P. van Duyne, T. J. Marks and P. C. Stair, *Angew. Chem. Int. Ed.*, 2015, **54**, 13346-13351.
22 R. Bhattacharyya and L. Frydman, *J. Chem. Phys.*, 2007, **127**.
23 E. Kupce and R. Freeman, *J. Mag. Reson. A*, 1995, **115**, 273-276.
24 L. A. O'Dell and R. W. Schurko, *Chem. Phys. Lett.*, 2008, **464**, 97-102.
25 K. J. Harris, A. Lupulescu, B. E. G. Lucier, L. Frydman and R. W. Schurko, *J. Magn. Reson.*, 2012, **224**, 38-47.
26 T. Kobayashi, F. A. Perras, T. W. Goh, T. L. Metz, W. Huang and M. Pruski, *J. Phys. Chem. Lett.*, 2016, **7**, 2322-2327.
27 D. A. Hirsh, A. J. Rossini, L. Emsley and R. W. Schurko, *Phys. Chem. Chem. Phys.*, 2016.
28 F. Alkan and C. Dybowski, *J. Phys. Chem. A*, 2016, **120**, 161-168.
29 L. Robinet and M. C. Corbeil, *Stud. Conserv.* 2003, **48**, 23-40.
30 M. J. Katz, P. M. Aguiar, R. J. Batchelor, A. A. Bokov, Z. G. Ye, S. Kroeker and D. B. Leznoff, *J. Am. Chem. Soc.*, 2006, **128**, 3669-3676.
31 J. Catalano, Y. Yao, A. Murphy, N. Zumbulyadis, S. A. Centeno and C. Dybowski, *Appl. Spectrosc.*, 2014, **68**, 280-286.

32 A. Zagdoun, G. Casano, O. Ouari, M. Schwaerzwalder, A. J. Rossini, F. Aussenac, M. Yulikov, G. Jeschke, C. Coperet, A. Lesage, P. Tordo and L. Emsley, *J. Am. Chem. Soc.*, 2013, **135**, 12790-12797.
33 R. K. Harris, E. D. Becker, S. M. C. De Menezes, P. Granger, R. E. Hoffman and K. W. Zilm, *Solid State Nucl. Magn. Reson.*, 2008, **33**, 41-56.
34 P. Martinetto, M. Anne, E. Dooryhee, P. Walter and G. Tsoucaris, *Acta Crystallographica*, 2002, **58**, I82-I84.
35 M. A. Verhoeven, L. Carlyle, J. Reedijk and J. G. Haasnoot, in *Reporting Highlights of the De Mayerne Programme*, eds. J. J. Boon and E. S. B. Frereira, NWO, 2006, pp. 33-42.
36 J. Catalano, Y. Yao, A. Murphy, N. Zumbulyadis, S. A. Centeno and C. Dybowski, *MRS Proceedings*, 2014, **1656**.
37 D. Massiot, I. Farnan, N. Gautier, D. Trumeau, A. Trokiner and J. P. Coutures, *Solid State Nucl. Magn. Reson.*, 1995, **4**, 241-248.
38 P. C. A. van der Wel, K.-N. Hu, J. Lewandowski and R. G. Griffin, *J. Am. Chem. Soc.*, 2006, **128**, 10840-10846.
39 O. Lafon, A. S. L. Thankamony, T. Kobayashi, D. Carnevale, V. Vitzthum, I. I. Slowing, K. Kandel, H. Vezin, J.-P. Amoureux, G. Bodenhausen and M. Pruski, *J. Phys. Chem. C*, 2013, **117**, 1375-1382.
40 A. J. Rossini, C. M. Widdifield, A. Zagdoun, M. Lelli, M. Schwarzwalder, C. Coperet, A. Lesage and L. Emsley, *J. Am. Chem. Soc.*, 2014, **136**, 2324-2334.
41 W. P. Rothwell and J. S. Waugh, *J. Chem. Phys.*, 1981, **74**, 2721-2732.